Paper presented at the 13th Int. Conf. on General Relativity and Gravitation
Cordoba, Argentina, 1992: Part 1, Plenary Lectures

Gravitational lensing

Jürgen Ehlers and Peter Schneider
Max–Planck–Institut für Astrophysik, Karl–Schwarzschild–Str. 1, W–8046 Garching, Germany

1. Introduction

1.1. Historical Remarks

In his Opticks, published in 1704, Sir Isaac Newton already asked: "Do not Bodies act upon Light at a distance, and by their action bend its Rays?" This question was taken up only in 1784 by Henry Cavendish and, independently in 1801, by Johann von Soldner. They both computed the bending of the orbits of "lights corpuscles" by a spherical body of mass M and found the "Newtonian" deflection angle

$$\hat{\alpha} = \frac{2GM}{c^2 r} = \frac{R_s}{r} \quad , \tag{1}$$

provided $r \gg R_s$ is the impact parameter and the photon's speed at infinity is c; R_s denotes what we now call the Schwarzschild radius of the deflecting body. At the time this prediction could not be tested and was apparently soon forgotten. The question of gravitational light deflection was raised anew by Albert Einstein. In 1907 he rediscovered the law (1) by combining heuristically Maxwell's equations with his principle of equivalence, which led to an effective index of refraction

$$n = 1 - \frac{U}{c^2} \tag{2}$$

of a vacuum gravitational field depending on the gravitational potential U. Finally, in 1915, in possession of his field equation, he noted almost in passing that space curvature doubles the bending, so that (1) and (2) have to be changed into

$$\hat{\alpha} = \frac{2R_s}{r} \quad , \quad n = 1 - \frac{2U}{c^2} \quad , \tag{3}$$

results now verified by VLBI to within an uncertainty of about 10^{-3}.

Sir Arthur Eddington (1920) and O. Chwolson (1924) realised that light deflection may cause several images ("fictitious binaries", e.g.) of a source, and Einstein (1936) computed the change of apparent brightness due to differential deflection by a point mass. The observability of such effects was considered very unlikely, though, due to the small probability for sufficient alignment of sources and deflectors, taken to be stars in our galaxy. However, in 1937 in two remarkably prescient papers Fritz Zwicky considered the possible astronomical importance of gravitational light bending by external galaxies and concluded that "the probability that nebulae which act as gravitational

lenses will be found becomes practically a certainty". Possible astrophysical and cosmological applications of gravitational lensing have been elaborated theoretically since the early sixties. At GR4, held in London in 1965, Sjur Refsdal showed, among other things, how masses of galaxies and the Hubble constant might be measured by lensing.

The first verification of Zwicky's prediction occured in 1979 when D. Walsh, R.F. Carswell and R.J. Weymann tentatively interpreted a "double quasar" as a pair of images of one quasar and within one year A. Stockton and P. Young *et al* identified the lensing galaxy. Since then at least 7 firm cases of multiply imaged quasars and about 20 gravitationally lensed images (arcs, rings) of galaxies or radio lobes of quasars have been found. Theoretical activity has, of course, increased rapidly in connection with these discoveries.

1.2. The astrophysical significance of lensing

Gravitational lensing may serve to

- determine masses of galaxies and clusters and the distribution of matter in them, including dark matter;
- explain luminous arcs and rings;
- observe distant sources, magnified by gravitational lenses which act like (cheap) telescopes;
- estimate sizes of Ly–α clouds.

By microlensing, one may

- identify dark deflection bodies;
- measure the size and structure of different emission regions particularly of QSOs;
- study the graininess (stellar population) of deflecting systems.

Successful models of gravitational lens cases also serve to confirm our picture of the universe, especially the cosmological nature of QSO redshifts. Moreover, taking into account statistically the light deflection caused by inhomogeneously distributed matter provides corrections to the ideal observable relations of Friedmann universe models. Finally, such successful applications provide evidence, if only indirect one, for the validity of the law of gravity on galactic and supergalactic scales.

This brief report outlines the theoretical framework and describes some of the applications of the, by now quite extensive, field of gravitational lensing, with emphasis on the role of GR. For more details and references, we refer to a forthcoming book (Schneider, Ehlers and Falco 1992, hereafter SEF), the conference reports Moran, Hewitt & Lo (1992), Mellier *et al* (1990), Kayser & Schramm (1992), the contributions by Blandford and Fort to GR12, and the excellent review article by Blandford and Narayan (1992). The notation here follows that of SEF.

2. Theoretical framework

2.1. From Maxwell's equation to geometrical optics; Fermat's principle in GR

A locally approximately plane electromagnetic wave in an arbitrary spacetime obeys, in leading WKB order, Maxwell's vacuum field equations if and only if

$$F_{\alpha\beta} = 2R\left\{e^{iS} k_{[\alpha} A_{\beta]}\right\} \quad ,$$

where

$$k_\alpha = S_{,\alpha} \quad , \quad g^{\alpha\beta} S_{,\alpha} S_{,\beta} = 0 \quad , \tag{4a}$$

$$k^\alpha A_\alpha = 0 \quad , \quad k^\beta A_{\alpha;\beta} = -\frac{1}{2} A_\alpha k^\beta{}_{;\beta} \quad . \tag{4b}$$

According to the eikonal equation (4a) for the (real) phase S, the light rays, defined as integral curves of $\dot{x}^\alpha = k^\alpha$, are null geodesics; (4b) says that the (complex) amplitude A_α is transverse, $k^\alpha A_\alpha = 0$, and propagates along the rays such that the polarization vector is parallel on the rays and $-A^*_\alpha A^\alpha$ changes inversely to the area of the cross section of an "infinitesimal" ray bundle. The energy tensor of such a wave, averaged "over a wavelength", behaves like that of a stream of "photons" with 4–momentum $\hbar k^\alpha = P^\alpha$ and conserved 4–current number density $N^\alpha = -(2\hbar^2)^{-1} P^\alpha$; $T^{\alpha\beta} = N^\alpha P^\beta$. A radiation field may be represented classically either as a photon gas or as an incoherent ensemble of waves. It then further follows that I_ω/ω^3, where I_ω is the specific intensity and ω the circular frequency, is an observer independent invariant which is constant on each ray if there is no interaction with matter.

For gravitational lens theory, the most useful way to characterise light rays is in terms of the following version of Fermat's principle, due essentially to H. Weyl (1917!):

In a conformally static spacetime with metric ($c = 1$)

$$ds^2 = \Omega^2 \left\{ e^{2U} d\eta^2 - e^{-2U} dl^2 \right\} \quad , \tag{5}$$

where the scalar U and the Riemannian 3–metric dl^2 depend on the spatial coordinates only — the conformal factor $\Omega > 0$ may depend on all coordinates — a spacetime null curve $x^\alpha(u)$ is a geodesic if and only if its spatial projection $x^a(u)$ obeys the variational principle

$$\delta \int e^{-2U} dl = 0 \quad ; \tag{6}$$

the variation is to be done with fixed end points. Since $\eta_a = \int e^{-2U} dl$, according to (5), is the arrival time of a photon emitted at $\eta = 0$, (6) expresses the stationarity of the arrival time η_a. (For a generalisation to arbitrary spacetimes, see Perlick 1990 and SEF.)

The foregoing statements about light rays, polarization vectors and intensities, combined with approximations and statistics, form the basis of gravitational lens theory.

2.2. Time delay and Fermat potential

Let some domain of spacetime contain a point source S, a point observer O and, between S and O, a matter distribution D, small compared to the distances of D from S and O. Because of light deflection by D, O may possibly see several images of S, and if the luminosity of S changes, this change might be noticed by O in the various images at different times. The observer may be able to measure the angles between the images and between the images and D, the fluxes of the various images, the redshifts of S and D, the spectra and polarisations of the light, and the time delays between images. For an extended source, O may also observe the shapes of the images of S. One basic task of lens theory is to establish relations between (i) the observables just listed, (ii) a model of D, and (iii) a model of the universe as far as it affects those relations.

To do this requires obviously more or less drastic approximations. The least problematic one is the use of geometrical optics (reasons for this are given, e.g., in SEF). To proceed, we assume the metric to be approximated, in the relevant part of spacetime containing the light rays from S to O, by (Futamase 1989, Jacobs *et al* 1991)

$$ds^2 = R^2(\mu)\left\{(1+2U)\,d\eta^2 - (1-2U)\,dl_k^2\right\} \quad , \tag{7}$$

where dl_k^2 is a metric of constant curvature, $k = 1, -1, 0$, R the expansion function of a "background" Friedmann cosmological model with conformal time η, and U the (Newtonian) gravitational potential of the deflecting, localized matter D. Except for some neighbourhood of D, $U \ll 1$, and (7) is nearly a Robertson–Walker metric. During the time light passes D, R and U are nearly constant, and in the region where most of the deflection takes place, dl_k^2 is nearly Euclidean, so there (7) reduces to the linearized metric of a weak source. It is, then, reasonable (and usual) to assume that the relevant light rays proceed from the source to the neighbourhood of D as in the background, get deflected and retarded near D, and then proceed undisturbed to the observer.

The metric (7) is conformally static, thus Fermat's principle applies. To use it, we consider null curves consisting of two smooth, geodesic pieces, one from the source to an event D near the deflector, and one from there to the observer, with a corner at D. Their projections into the "comoving" 3–space with metric dl_k^2 are spatial geodesics with lengths l_d, l_s, l_{ds}, see Fig. 1.

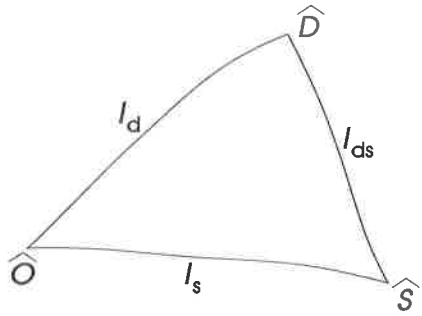

Figure 1.

$\hat{O}$, $\hat{S}$, $\hat{D}$ are the points in the comoving space representing O, S, D. The unperturbed path proceeds smoothly from $\hat{S}$ to $\hat{O}$, of course.

On each ray, since $ds^2 = 0$, we have by (7) $\int d\eta = \int dl - 2\int U dl$. Measured in proper time at the observer when $R = R_0$, the arrival time delay Δt of the broken ray relative to the unperturbed ray is therefore

$$\Delta t = R_0 \Delta\eta = R_0(l_d + l_{ds} - l_s - 2\int U dl) \quad .$$

With a little trigonometry, the Newtonian expression for U and the assumption that the deflector is transparent and geometrically thin (SEF), one arrives at a formula for the arrival time delay:

$$\Delta t = \frac{(\vec{\theta} - \vec{\beta}^2)^2}{2H_0\,(\chi_d - \chi_s)} - 2R_s\,(1+z_d)\,\Psi\,(\vec{\theta}) + \text{const.} \tag{8}$$

$\vec{\theta}$ denotes the (vectorial) angular distance of an image from the center of D, $\vec{\beta}$ the (unobservable) angular distance of the unperturbed source from the deflector, H_0 the Hubble constant, R_s the Schwarzschild radius of the deflector and

$$\Psi(\vec{\theta}) = \int \frac{dm'}{M} \ln\left|\vec{\theta} - \vec{\theta}'\right| \tag{9}$$

is a deflection potential, here defined in terms of the fraction $\frac{dm'}{M}$ of mass of D contained in a solid angle $d^2\theta'$.

The χ–terms in (8) arise as follows. The auxiliary distances l in Fig. 1 can be related to angular diameter distances D_d, D_s, D_{ds} as defined in the background universe of eq. (7). They are also unobservable, theoretical quantities. To relate them to the observable redshifts of source and deflector, z_s and z_d, one has to specify how the metric of the inhomogeneous universe is to be split into a background part and a perturbation. One way of doing this is to assume that, on average, the expansion rate of the actual universe (on the scale, say, of galaxies) equals that of the background Friedmann universe, $\langle\theta_{\text{inh.}}\rangle = \theta_F$, and $\langle\dot{u}^\alpha_{\text{inh.}}\rangle = 0$ ($\dot{u}^\alpha$ = 4–acceleration), and that the averaged area $\int dA_{\text{inh.}}$ of a cross section z = const. of a typical past light cone equals that of the background universe. Let ϱ_b be the density of that background, and let the fraction $\tilde{\alpha}$ of all mass be distributed smoothly, so that the factor $1 - \tilde{\alpha}$ is bound in clumps. The angular diameter distance will then refer to "empty cones", i.e. to ray bundles between clumps where the density is $\tilde{\alpha}\varrho_b$; these D's are called Dyer–Roeder distances. Then one gets the useful relation (SEF)

$$(1 + z_d)\,\frac{D_d D_s}{D_{ds}} = \frac{c}{H_0}\,\left[\chi_d - \chi_s\right]^{-1} \quad , \tag{10}$$

where $\chi(z; \Omega, \tilde{\alpha})$ is a function of $\tilde{\alpha}$, the present density parameter Ω, and the redshift and $\chi_d \equiv \chi(z_d; \tilde{\alpha}, \Omega)$ etc. This equation has been used to obtain (8).

The function $\Delta t(\vec{\theta}, \vec{\beta})$ clearly exhibits the influence of the lens (Ψ, R_s) and of the cosmological model (H_0, χ) on the time delay and thus of the lens mapping (see below); it deserves the name Fermat potential.

2.3. The lens mapping and related equations

Eq. (8) is valid for all kinematically conceivable, broken light rays. The actual, physical light rays follow via Fermat's principle, (6), which here gives $\frac{\partial}{\partial\vec{\theta}}\,\Delta t = 0$, hence

$$\vec{\beta} = \vec{\theta} - 2R_s H_0\,(1 + z_d)\,(\chi_d - \chi_s)\,\frac{\partial\Psi}{\partial\vec{\theta}} \quad . \tag{11}$$

It can be used to express angular distances between several images of a source in the form

$$\vec{\theta}_{ij} = \vec{\theta}_i - \vec{\theta}_j = g(z_d, z_s, \Omega, \tilde{\alpha})\,R_s H_0\,(\vec{\alpha}(\vec{\theta}_i) - \vec{\alpha}(\theta_j))$$

where $\vec{\alpha} = 2\,\frac{R_s}{D_a}\,\frac{\partial\Psi}{\partial\vec{\theta}}$ is the deflection angle. Moreover, using (11) in (8), one gets

$$\Delta t_{ij} = 2R_s\,(1 + z_d)\,h\,(\vec{\theta}_i, \vec{\theta}_j) \quad .$$

In the last two equations, g depends on the cosmological model, and h and $\vec{\alpha}$ depend on the deflector model. These equations show how, in principle, the deflector mass or R_s, H_0, Ω, $\tilde{\alpha}$ can be obtained from lens observations, provided one has a reliable model for the relative mass distribution in the lens. In practice, many difficulties have to be overcome (see the references cited).

2.4. Two general theorems, magnification

The lens mapping

$$f : \mathbb{R}^2 \to \mathbb{R}^2 , \quad \vec{\theta} \to \vec{\beta} \tag{12}$$

given by eq. (11) is, for localized lenses, invertible for large $\vec{\theta}$. In general, however, $f^{-1}(\vec{\beta}) = \left\{\vec{\theta}_1, \ldots, \vec{\theta}_{2N+1}\right\}$; the number of images is odd (Burke 1981). The inverse μ_{ij} of the Jacobian matrix

$$\beta_{ij} = \frac{\partial \beta_i}{\partial \theta_j}$$

describes the distortion of an image compared to that of the undistorted source which, of course, is not observable. However, the μ_{ij} at several images can be composed to give the relative distortion of the images.

Since lensing does not change the frequencies, constancy of I_ω implies that the flux magnification (relative to the unlensed case) is given by the absolute value of

$$\mu = \det \ \mu_{ij}$$

while sgn μ gives the parity of an image. In the case of transparent lenses, at least one image (with positive parity) is not demagnified, $\mu \geq 1$; generically $\mu > 1$ for at least one image (Schneider 1984).

2.5. Critical curves and caustics

Rescaling the variables $\vec{\beta}$, $\vec{\theta}$, one may rewrite the lens mapping (11) as

$$f : \vec{x} \to \vec{y} = \nabla \left(\frac{1}{2} \vec{x}^2 - \Psi (\vec{x}, \vec{p}) \right) \quad . \tag{13}$$

Here, $\vec{p}$ denotes parameters on which a lensing configuration may depend.

Alternatively, the source position $\vec{y}$ corresponding to an image $\vec{x}$ can be characterized by

$$\nabla \phi = 0 , \quad \phi = \frac{1}{2} (\vec{x} - \vec{y})^2 - \Psi (\vec{x}; \vec{p}) \quad . \tag{14}$$

(As before, the gradient operator refers to $\vec{x}$.)

To avoid confusion, we shall use the terminology appropriate to the *physical meaning* of the symbols; thus $\vec{y}$ is called the source position, $\vec{x}$ the image position (although according to mathematical terminology $\vec{x}$ is the pre–image, $\vec{y}$ the image variable for the map f defined by (13)).

One basic question of lens theory is: How many images exist for a given source, i.e. what is the set $f^{-1}(\vec{y})$, and how does it depend on $\vec{y}$? For localized sources the deflection potential Ψ increases like ln r, the deflection angle decreases like r^{-1}. Therefore,

as one would expect, the map f is bijective for large $|\vec{x}|$. Also, f is surjective, i.e. for any source position $\vec{y}$, there is at least one image $\vec{x}$ such that $\vec{y} = f(\vec{x})$. Thirdly, if the Jacobian matrix $\left(\frac{\partial \vec{y}}{\partial \vec{x}}\right)$ is invertible at $\vec{x}$, the map f is locally invertible at $\vec{x}$. Therefore, if $\vec{y}$ moves inwards from infinity along a curve, there will for a while be a unique image $\vec{x}$ until possibly a point is reached where $\det\left(\frac{D\vec{y}}{D\vec{x}}\right) = 0$. The set of all points $\vec{x}$ where this equation holds is called the *critical set*, its image the *caustic set* of f. In the theory of singularities of maps one studies the behaviour of f and f^{-1} near critical and caustic points, respectively, in general. Lens theory is concerned with the special case of *gradient maps*, see eq. (14).

One may study such maps from several points of view, two of which we mention.

Firstly, one may consider f as defining a 2–surface in $\mathbb{R}^4 = \{(\vec{x}, \vec{y})\}$. On this 2–surface, the sympletic form $\Omega = dy_i \wedge dx_i$ vanishes; thus the 2–surface is a Lagrangean submanifold of $(\mathbb{R}^4, \Omega)$. The lens map may then be viewed as a *projection* of this 2–surface onto the $\vec{y}$–plane. This is useful since it gives a "quasi–intuitive" insight into the way of how $f^{-1}(\vec{y})$ changes with $\vec{y}$, and since such *Lagrangean maps* have been studied extensively by mathematicians.

In the second view, based on (14), one thinks of $\vec{x} \to \phi(\vec{x}, \vec{y}; \vec{p})$, for each fixed value of the *control parameters* $(\vec{y}, \vec{p})$, as a surface in $(\vec{x}, \phi)$–space. For large $\vec{x}$, this arrival time surface approaches the paraboloid $\phi = \frac{1}{2}(\vec{x} - \vec{y})^2$. The images, in this context also called *states*, then correspond to those points where the tangent plane to the surface is parallel to the plane $\nabla\phi = 0$. (This second view corresponds to the so–called "static model" of catastrophe theory, which is popular also in discussions of phase transitions.)

By eqs. (13) and (14) the Jacobian matrix of the lens mapping has components

$$\frac{\partial y_i}{\partial x_k} = \phi_{ik} = \delta_{ik} - \Psi_{ik} \quad .$$

Since for $x \to \infty$, $\Psi_{ik} \to 0$, the critical set is bounded and, of course, closed, hence compact. The caustic set is compact and in addition of measure zero (Sard's theorem).

At a regular, i.e. non–critical image $\vec{x}^{(0)}$, the magnification μ is finite, and near $\vec{x}^{(0)}$, f is locally diffeomorphic. At a critical image $\vec{x}^{(0)}$, the magnication is formally infinite; however, if instead of a point source an extended source is considered or if wave optics is taken into account, the "physical" magnification becomes finite, but in general large.

It follows from the above that if $\vec{y}$ moves, the number of its images can change only if $\vec{y}$ enters or crosses the caustic set. Thus knowing the critical and caustic sets provides a qualitative overview of a lens mapping.

Generically, the critical set of a lens mapping consists of finitely many closed, smooth, compact curves without end points. The images of critical curves, the caustics, may have finitely many *cusps* (spikes).

Whenever a source point crosses a caustic where the latter is smooth, two new images appear on opposite sides of the critical curve; the corresponding segments of critical curves which consist of "double images", are called *folds*. Near and inside a cusp, a source point has three images which merge when the source reaches the cusp, and only one image survives if the source has passed through the cusp. Both folds and cusps are stable, i.e., they are preserved under all small deformations of the deflection potential, and smooth maps $\mathbb{R}^2 \to \mathbb{R}^2$ have no other kinds of stable singularities than folds and cusps (Whitney 1955). Near a fold, the amplification diverges like the inverse square root of the distance from the caustic; near a cusp, it diverges even stronger.

These facts can be established by approximating the Fermat potential at a critical point by a polynomial of suitably high order and then studying the resulting representative mapping.

If one considers not a single lens mapping, but a family of those depending on some parameters $\vec{p}$, the critical curves and caustics depend on the value of $\vec{p}$. Qualitative changes of the pattern of critical curves and caustics, called *metamorphoses*, can occur for particular values $\vec{p}^{(0)}$ and at special points $(\vec{x}^{(0)}, \vec{y}^{(0)})$. These higher–order singularities are also useful to survey lensing models; they are needed to study caustics and self–intersections of null cones of spacetimes, but we shall not pursue this topic here, but refer the reader to Chap. 6 of SEF (see also Blandford & Narayan 1986).

2.6. Remarks on mutliple lens plane theory

The theory outlined so far effectively deals with cases where, because of the thin–lens assumption and small deflection angles, the lensing matter may be thought of as being distributed on a single lens plane between source and observer. Instead, one may consider the more general case where several such lens planes occur (Blandford *et al* 1986, Kovner 1987, SEF), an idealisation which better approximates the real situation where clumps at all redshifts influence light propagation.

The resulting mapping may again be obtained via Fermat's principle. It is, of course, more complicated than the single plane case. In particular, in contrast to (14) the mapping is no longer a gradient map. (Question: is it still Lagrangean?) The odd number theorem remains valid, and recently it has been shown that this also holds for the magnification theorem stated in 2.4 (S. Seitz *et al* 1992).

3. Remarks about the observational situation

Gravitational lens phenomena, predicted long ago, have been observed in a variety of appearances. First, there are cases of strong lensing; by that we mean that a deflector is sufficiently massive and compact to split images of a background source, or at least to distort them in such a way that the lens phenomenon is readily identified or at least suspected. Examples of strong lensing are multiply imaged QSOs, the luminous arcs in clusters of galaxies, and the radio rings.

In contrast to strong lensing, weak lensing cannot be identified in individual sources, but only by considering a sample of sources. For example, background galaxies are distorted by a foreground cluster in a characteristic way (images are preferentially elongated in a direction tangent to the cluster center). However, since galaxies are not intrinsically round, the distortion cannot be identified from any individual galaxy image, but only the statistical analysis of the images of background sources around a cluster yields evidence for the coherent image distortion. Weak lensing particularily means that the magnifications of the images are not very much larger than unity.

A third class of lensing phenomena is microlensing: light bundles from distant compact sources 'feel' the graininess of the matter distribution in intervening galaxies. The stars in such galaxies cause only small deflections, but their differential deflection can be sufficient to yield considerable magnification.

This is not the place to provide an – even only partially – complete review of observed lensing phenomena and specific objects; the reader is referred to the reviews mentioned

in the introduction, and to the report by Fort (1990) from the last GR conference and references therein. Instead, we will pick out a few aspects which may be of particular interest to relativists.

3.1. Multiple QSOs

Up to now, we know about seven firm cases of multiply imaged QSOs, and about as many good candidates for this effect. The criteria by which a candidate lensing system becomes a secure case of lensing are not easily explicitly stated, but having two QSO images with the same redshift and similar spectra is not sufficient to enter the class of lens system. In fact, the lensing community has learned its lesson from objects like 1145−071, where two closely spaced QSO images have the same redshift, similar spectra, but only one of them is a strong radio source, with very strict limits on the radio flux ratio. Although one could construct complicated (and artificial) lens models which account for the observations, this system most likely is a binary QSO, rather than a lensed source. In order for a multiple QSO to be accepted as a lens system, one or more of the following criteria should be satisfied in addition to the similarity of spectra: (a) in the case of two images, (a1) they both should be radio QSOs, and the radio characteristics should agree (spectral slope, morphology in resolved sources), (a2) a potential lens should be seen between or near the images, (a3) both QSOs should show other relatively rare properties, such as broad absorption lines, (correlated) rapid variability, high polarization etc. (b) If more than two images are seen, the lensing hypothesis becomes more probable a priori, in particular if the geometrical arrangement of the images is according to the expectations from 'generic elliptical' lens models.

The two doubles confirmed as lens systems both have a visible galaxy between the images; in addition, for 0957+561, both components are radio sources, and VLBI has revealed the similar milliarcsecond radio structure (also showing the different parities of the two images), which yields particularily striking evidence for the lensing nature of this system. For the one confirmed triple, 2016+112, there are several objects close to the images, two of which have been identified as galaxies (at different redshifts); in this case, light from the QSO is probably deflected more than once. The four known quadruples, the best-known of which is the so-called Einstein cross 2237+0305, have their images arranged in a form which is predicted by all canonical models, i.e., either rather symmetrically, in which case the images have comparable brightness, or two of the images are close together (as in the case of the so-called 'triple-QSO' 1115+080) and are much brighter than the remaining two, indicating that the close pair of images lies close to a critical curve of the lens. For 2237+0305 the lens is easily observable (this lens system will be discussed in more detail below), and the lens in 1115+080 has also been found. The image separation of these multiply imaged QSOs range from slightly more than one arcsecond to about six arcseconds.

Except for 2016+112, a case which is theoretically not well understood, all multiply imaged QSOs have an even number of images, in contrast to the theoretical expectation mentioned in Sect.2.4. However, the odd number theorem made no prediction about the relative brightnesses of the images. It is currently believed that the 'missing image' is very close to the center of the lensing galaxy where the surface mass density is so high as to yield a strong demagnification (overfocusing) of this central image. In fact, none of the multiple QSO lens systems yields a hint of a finite core radius of the lens.

There are several candidates for multiply imaged QSO, mostly doubles (since for them verification is most difficult). Perhaps the most interesting case is 2345+007, a

double QSO with 7.3 arcsecond separation, the largest known. Spectral similarities are striking; the report (Nieto et al 1988) that one of the images is indeed a close double has not been confirmed by other groups. No sign of any lens has been obtained in deep imaging of the field; however, a strong absorption line system at redshift 1.49 indicates matter in the lightbeam in one of the two images (that which is suspected as double). As will be discussed below, clarification of the lensing nature of 2345+007 is of vital importance for an application to the determination of intervening Lyα clouds. The status of the double system 1635+267 ($\Delta\theta = 3.8$ arcseconds) is similar to that of 2345+007: the spectra of both images are remarkably similar, and this system is an excellent candidate for lensing. Recently, a very close pair ($\Delta\theta \approx 0.45$ arcseconds) has been identified, both through ground-based observations (Magain et al. 1992) and from the Space Telescope gravitational lens snapshot survey (Maoz *et al* 1992); the QSO has a redshift of 3.8, making it the lens candidate with the largest redshift. The small image separation observed in that system is close to the most probable separation as expected from theory, if standard assumptions about the distribution of galaxies in the universe (i.e., the lens population) are made.

3.2. Rings

From symmetry, if a source is situated behind a (sufficiently compact) spherical deflector, its image will be a ring. However, exact symmetry is not needed for the formation of ring-shaped images, if extended sources are considered. Five ring images have been found to date (see contributions in Kayser and Schramm 1992), all by radio observations. In the first case (1131+0456), optical imaging suggests a similar ring-like structure for the optical source (Hammer & LeFevre 1991), but the best argument in favour of lensing is detailed modeling: since the image of an extended source contains much more information than a few point images, typical lens models for rings are highly overdetermined. The reconstruction of the image from a simple lens model, applied to data in two wavebands and to the polarized flux, provides a powerful tool not only to constrain lens parameters (such as mass and ellipticity), but also to confirm the lensing nature (Kochanek *et al* 1988); recently, this inversion technique has been greatly improved to account for finite resolution maps (Kochanek & Narayan 1992). For a second ring, MG1654+1346, the lensing nature is indisputable: one of the two radio lobes of a QSO at redshift 1.7 is mapped into a ring image by a galaxy at redshift 0.25, centered on the ring. A third ring source, PKS1830−211, one of the strongest radio sources in the sky, contains two compact components which are rapidly variable; monitoring of this source and detailed modeling could make this an ideal target for applying the lens method to determine the Hubble constant (see below).

3.3. Arcs and arclets

In about 10 clusters of galaxies, long and narrow images (arcs) have been observed. Whereas the nature of these images has been controversial right after their discovery, the redshift measurement of one of these arcs have ruled out interpretations which put the arc at the same redshift as the cluster. Several such redshift measurements are available today, all with higher values than the cluster in which the arc is seen.

Presently, the nature of the arcs is interpreted as galaxies at high redshift being gravitationally lensed by foreground clusters. The highly elongated shape of the images

is due to the distortion by the lens mapping, with the source being situated close to a cusp singularity of the lens. (There are also "straight arcs", which are most conveniently interpreted as sources lying close to so-called beak-to-beak singularities, one of the types of metamorphoses mentioned in Sect. 2.5.) Note that the length of the arc in A370 is about 21 arcseconds, and its width is roughly 2 arcseconds, so that the deformation by lensing is indeed huge; correspondingly, the total flux of the image is much larger than that of the unlensed source. It is only this high magnification which allows spectroscopy of such intrinsically faint extended sources – clusters of galaxies forming arcs provide us with (cheap) 'natural telescopes'.

If a cluster is sufficiently compact to form such spectacular long arcs, it will also deform other background sources lying close to the direction to the center of the cluster. One example of this effect can be seen in A370, where various elongated blue images are observed. These images share the property that they are elongated in the tangential direction with respect to the cluster center. Such tangential elongation is expected from light deflection. Indeed, the redshift of one of these arclets in A370 has been measured to be $z_s = 1.305$ which thus stems from a background source. Since the density of faint background galaxies is very large (Tyson 1988), these sources can in principle be used to 'map' the mass distribution of compact clusters. This is not a trivial task, both from observation and theory. Very deep images have to be obtained in order for the source density to be sufficiently high. Sources (galaxies) are intrinsically not round, and therefore intrinsic ellipticity has to be disentangled from lens-induced deformation. This clearly is an ambitious statistical problem, treated in considerable depth in the literature (e.g., Kochanek 1990, Miralda-Escudé 1991), but has been demonstrated to work in practice (Tyson, Valdes & Wenk 1990), thus constituting a nice example of weak lensing. In principle, the redshift distribution of this faint background galaxy population can be obtained from such studies of arclets around a sample of clusters of galaxies.

3.4. Microlensing

The graininess of the matter in galaxies affects the light bundles of sufficiently small sources traversing such a galaxy. The relevant scale for the source is about $3 \times 10^{16} \sqrt{M/M_\odot}$ cm, so that the optical (and X-ray) continuum emission from AGNs can be affected by this effect, whereas the broad line region is probably too large to be affected as a whole (differential effects, however, affecting the shape of the broad emission lines, can occur). Since the relative alignment of source and lensing galaxy changes in time, so does the magnification: microlensing leads to a lens-induced variability of sources seen through a galaxy. This effect, in general, is extremely difficult to distinguish from intrinsic variability of sources, but for multiply imaged QSOs, such microlensing could be observed: an intrinsic variation of the source will be seen in all images, with their respective time delay, whereas variability due to microlensing is uncorrelated between the individual images.

The best lens system for observing microlensing is 2237+0305, owing to the small redshift ($z_d \approx 0.04$) of the lens (so that velocities in the lens plane correspond to large effective velocities in the source plane) and to the fact that the time delay of the images is of the order of one day, so that intrinsic flux variations of the source will be seen nearly simultaneously in all four images. In fact, uncorrelated flux variations in at least three images have been observed (Corrigan et al. 1991), ranging up to half a magnitude. This is a clear signature of microlensing.

It is relatively difficult to obtain quantitative conclusions from such microlensing observations. One can compare observed lightcurves with numerical simulations (see Wambsganss 1990 and references therein), but due to the statistical nature of the effect definite conclusions will only be possible if a sample of microlensing events is observed, which means that a sufficiently long data track of the source must be available. Nevertheless, the observations of microlensing in 2237+0305 have led to the following conclusions: the observed flux variations are compatible with the picture in which microlensing is produced by a normal stellar mass spectrum (Wambsganss, Paczyński & Schneider 1991, Witt, Kayser & Refsdal 1992). The size of the emission region of the optical continuum source of 2237+0305 is just compatible with a simple accretion disc model (Rauch & Blandford 1991, Jaroszyński, Wambsganss & Paczyński 1992); the observed variations lead to an upper limit of the source size.

In addition, microlensing can be used to obtain information about the brightness structure of sources. For example, the lightcurve of an extended source crossing a caustic is a convolution of its one-dimensional brightness profile and a universal function, the point-source magnification function near folds. Hence, from a well-observed high-magnification event in an observed microlensing light curve, the one-dimensional brightness profile of a source could in principle be reconstructed (Grieger 1990). The broad-line region in QSOs, probably too extended to be magnified as a whole by microlensing, has intrinsic structure. Therefore, differential magnification across the broad line region can affect the line profiles of the broad emission lines (Schneider & Wambsganss 1990). In fact, line profile differences in 2237+0305 have been observed by Fillipenko (1989). For further applications of microlensing, see Sect. 12.4 of SEF.

4. Applications of gravitational lensing effects

As mentioned before, gravitational light deflection does not only lead to spectacular effects as multiple images and rings, but has become a useful tool for astrophysics. Here, we want to mention only some of the potential applications which have been suggested in the literature, concentrating on those which might interest the cosmologists most.

4.1. Determination of the Hubble constant

As suggested as early as 1964 by S. Refsdal, the difference in light travel time between any two images of a multiply imaged QSO can be used to determine, at least in principle, the Hubble constant, i.e., the overall scale of a gravitational lens arrangement (from dimensional arguments, $H_0 \propto 1/\Delta t$). The only lens system which is sufficiently intrinsically variable and sufficiently monitored by now to detect correlated flux variations in both images (with a respective time delay) is 0957+561, but even in this system it has been extremely difficult to measure Δt. Only recently, by using a sophisticated statistical method applied to optical and radio data (Press, Rybicki & Hewitt 1992a,b) a reliable estimate has been obtained, $\Delta t = 540 \pm 12$ days. The correlation of flux of both images is not perfect, indicating that at least one of the images is affected by microlensing (Schild & Smith 1991).

The determination of the Hubble constant from the measurement of the time delay, as discussed above, requires knowledge about the mass distribution of the lens. However, in this respect the system 0957+561 is a fairly complicated one, since the cluster

in which the main lensing galaxy is embedded makes a significant contribution to the deflection. Unfortunately, basically nothing is known about the mass distribution of the cluster. The construction of lens models proceeds by assuming that the deflection caused by the cluster varies slowly over the region of the size of the image separation; the contribution by the cluster is then described by the lowest order terms of a Taylor expansion of the deflection angle around the center of the main galaxy (the validity of this approach can be questioned, see Kochanek 1991a). A 'plausible' ansatz for the shape of the mass distribution in the lens galaxy is chosen, compatible with what is known about the matter distribution in elliptical galaxies, and the parameters of the model are varied to obtain a match of all observables with the model. Needless to say that such an approach yields models which are far from being unique. Even worse, there are invariance transformations of lens model parameters which have no impact on the observables (Gorenstein, Falco & Shapiro 1988; e.g., adding a uniform mass sheet to the lens acts like a Gaussian thin lens and is equivalent, in terms of the lens model, to decreasing the separation between lens and source). This degeneracy can be broken by obtaining additional observables; in the case of 0957+561, the velocity dispersion of the lens galaxy (a measure for the lens mass) has been observed, thus allowing the degeneracy to be broken. It thus seems that a point estimate of the Hubble constant is possible from this lens system. Taking the lens model from Falco, Gorenstein & Shapiro (1991), assuming that the velocity dispersion measures the total mass of the lens galaxy, and taking a cosmological model with $\Omega_0 = 1$, one obtains a value for H_0 which is less than $50\,\mathrm{km\,s^{-1}\,Mpc^{-1}}$ (the 'best' value being closer to 40). The uncertainties, however, are still considerable. First, as already mentioned, the lens model is not unique, and one can construct equally good models which would yield different values for H_0. Second, it is not clear whether the velocity dispersion of the stars probes the total matter of the lens galaxy; if the stellar mass is more centrally concentrated than the dark matter in the galaxy, the effective dispersion can be larger than the measured value by up to a factor $\sqrt{1.5}$. Third, additional inhomogeneities around the line-of-sight to the QSO can perturb the propagation of light and thus affect the lens mapping; in this respect it is interesting to know that spectroscopy of the galaxies around 0957+561 indicates that they do not all belong to a cluster at $z_d = 0.36$, but that there seems to be an additional concentration at a higher redshift of about 0.54.

With all the difficulties and uncertainties mentioned, it might appear that the determination of the Hubble constant from lensing will not yield more accurate values than the classical method of 'climbing up the distance ladder'. However, it should be stressed that the latter method measures the Hubble constant from nearby objects, whereas lensing permits to obtain measurements of H_0 on truly cosmic scales. It is by no means evident that both methods should yield the same results, in fact: since the probability that a galaxy (on which an observer is situated to measure H_0) is placed in an overdense region of the universe is high, the local Hubble expansion is likely to be slower than the mean Hubble expansion, yielding a systematically higher value of H_0 from local measurements. This was demonstrated quantitatively by Turner, Cen & Ostriker (1992). Hence, measuring H_0 from lensing might provide one of the few ways to obtain that value of H_0 which enters the Friedmann equations.

4.2. Constraints on the cosmological constant

Gravitational lensing provides a method to constrain the magnitude of a possible cosmological constant. Three different approaches have been used to obtain such con-

straints: as pointed out by Gott, Park & Lee (1989), the lensing behaviour of galaxies changes drastically if the cosmological constant is so large as to have an antipode at a redshift smaller than that of the source in a lens system. The confirmed lens system with the highest redshift ($z_s = 3.27$) is 2016+112, which implies that $q_0 > -2.3$; this estimate can be improved once lens systems with sources at higher redshifts are confirmed.

A positive cosmological constant λ increases the volume elements corresponding to a fixed redshift interval and solid angle. Assuming no strong evolution of the number and mass distribution of galaxies, the probability for any given source to be multiply imaged can be calculated as a function of source redshift and λ. Lensing probabilities become very large once λ approaches unity (for flat universes, i.e., $\Omega_0 + \lambda = 1$; see, e.g., Fukugita & Turner 1991, Fukugita *et al* 1992). Whereas existing lens surveys are burdened with selection biases (e.g., Kochanek 1991b), it seems unlikely that the results obtained so far are compatible with large λ cosmologies.

The effect of λ on the volume per redshift element depends on z. If a multiply imaged QSO is selected without regards to a lens (thus excluding systems like 2237+0305 for which the discovering observation was targeted to the lens galaxy), one can calculate the probability distribution for the lens redshift, which depends on λ; in particular, the probability is shifted towards larger redshifts of the lens for increasing λ. From available data, a large λ model can nearly be ruled out, and a few more lens systems adequate for this test can yield strong constraints on λ (Kochanek 1992). Note that these statistical effects are much more sensitive to λ than to Ω_0. However the uncertainties in lensing statistics are considerable (e.g., Mao 1991).

4.3. Mass distribution in lenses

Modeling an observed lens system yields values of the parameters of a parametrized lens model. Needless to say that there are many possible choices for the lens parameters, and so values obtained for physical parameters are not unique. The question is whether there are some physical parameters which are robust against variations of the parametrization of the lens model.

For double QSOs, there is not much we can learn about the matter distribution of the lens without a priori assumptions about its characteristics. An example of this can be found in Borgeest (1986). What is fairly well determined is that part of the mass of the lens which lies in a cylinder with axis along the line-of-sight and with radius being the mean of the angular separations of the two images from the center of the lensing galaxy (this mass estimate includes the mass from, e.g., a cluster in which the main lens galaxy is embedded).

The situation improves if quadruple QSOs are considered. In that case, the mass of the lens lying within a cylinder with radius being the mean of the separation of the images from the lens center is well determined. The best example of this is again 2237+0305: Observations with Space Telescope have revealed the image positions to very high accuracy. On the other hand, the closeness of the lens allows a detailed map of its brightness distribution. Assuming a constant mass-to-light ratio (M/L), surface brightness is directly translated into surface mass density. As has been shown recently (Rix, Schneider & Bahcall 1992), the assumption of constant M/L, i.e., a model with just three parameters (the other two being the unknown source position), is able to reproduce the positions of the images (8 observational constraints!) to within very

high accuracy. From that we can conclude that a constant M/L is a good assumption for this lens galaxy, and its value agrees with that obtained from stellar dynamics for 2237+0305 (Foltz *et al* 1992) and for other galaxies. The mass within the inner kpc of this galaxy is found to be $(2.16 \pm 0.04) \times 10^{10} M_{\odot}$ for a Hubble constant of 50, i.e., accurate to within 2%. This model reproduces the observed brightness ratios of the images only to within a factor of 1.5, which however is not surprising, since the flux of the images has been observed to be affected by microlensing.

For ring images, detailed reconstruction can yield fairly good estimates of the mass within the ring and the orientation and ellipticity of the mass distribution. The observational predictions of such lens models are very insensitive to the distribution of the matter inside the ring and nearly unaffected by the matter outside the ring.

Detailed modeling of arcs in several clusters of galaxies has provided us with some crucial information about the mass distribution in clusters: First, the amount of dark matter, inferred previously from studies of the dynamics of cluster galaxies, agrees with that obtained from the lens models (as is the case for galaxy-mass lenses, lens models for arcs are far from unique, with the mass inside a circle of radius given by the distance of the arc from the center of the cluster being the most robust parameter). Second, the dark matter is not tied to individual galaxies, but spread more evenly throughout the clusters. Third, the mass inside clusters of galaxies must be distributed more compactly than previously thought; otherwise, clusters would not be able to form caustics and thus multiple images. Once a complete sample of clusters (selected, say, by their X-ray flux; it seems that the X-ray luminosity of a cluster is a good indicator of its lensing power) is scrutinized for the occurrence of arcs, statistical information about the mass spectrum of clusters, their core radii etc. will be available (see Bergmann 1992, Wu and Hammer 1992).

4.4. Dark matter in our Galaxy

The rotation curve of our Galaxy and that of other spirals indicates the presence of dark matter. It is unclear what the nature of this dark matter is; candidates are: weakly interacting elementary particles, brown dwarfs and 'Jupiters', or black holes. If the dark matter is composed of such compact objects, these can lead to lensing effects of background sources: for stellar mass lenses, the corresponding angular separation of split images would be much too small to be detectable, but the magnification could be observed. The problem with this idea is that the probability of finding a single lens sufficiently close (within its Einstein radius) to the line of sight of an extragalactic object is about 10^{-6}. Hence, for observing this effect a huge number of sources must be photometrically monitored.

Paczyński (1986) suggested monitoring of the stars of a nearby galaxy, the Large Magellanic Cloud or M31. In fact, two groups are currently carrying out such an observational program (see the corresponding contributions in Kayser & Schramm 1992). The difficulties for such a program are enormous; we want to mention only a few of them. First, many stars are intrinsically variable, and it will be a major task to separate intrinsic variability from lens-induced one. A magnification event will be a 'once in a lifetime' event, that is, events will not recur. The program will work by comparing the brightnesses of sources from consecutive observations. The required large number of stars implies that the amount of data produced in the course of the program will be huge.

On the other hand, such an experiment is probably the only way to clarify the nature of the dark matter in the halo of our Galaxy. It will be sensitive to compact objects of masses between $10^{-6}M_\odot$, set by the time resolution, and about $1M_\odot$, determined by the duration of the experiment (note that this is the relevant mass range for 'brown dwarfs': objects with mass smaller than $\sim 10^{-7}M_\odot$ will have evaporated during the lifetime of our galaxy, whereas objects with mass $\gtrsim 0.1M_\odot$ burn hydrogen and shine, see De Rujula, Jetzer & Masso 1992). Paczyński (1991) suggested a calibration experiment, to observe the galactic bulge stars. There, we know the minimum density of lenses along the line of sight (the normal disk population of stars), and the probability of lensing turns out to be quite similar to that of the halo. Hence, this calibration experiment can be used to test the sensitivity of the observational program, including the software for data analysis, and may detect a population of brown dwarfs in the disk. Whatever the outcome of the program will be, it certainly will produce the most useful database for stellar variability and is thus worth the effort.

4.5. Massive black holes in the universe

If some fraction of the matter in the universe is contained in compact objects (defined such that their mass lies inside their Einstein radius; note that even red giants are compact objects with this definition), lensing can in principle reveal such a cosmic population (Press & Gunn 1973). Compact objects with mass $\gtrsim 10^{11}M_\odot$ lead to image splitting with angular separation $\gtrsim 1$ arcsecond, and their density can be constrained by the fraction of multiple QSOs. This fraction is small (at least for normal QSOs; the apparantly most luminous ones can have a larger fraction of lens systems due to the amplification bias, see Sect. 12.5 of SEF) and can be accounted for by the normal galaxy population (within all the uncertainties mentioned). Certainly, a mass fraction $\Omega \gtrsim 0.01$ in compact objects with mass $\gtrsim 10^{12}M_\odot$ can be excluded from existing data. The Space Telescope snapshot survey will be most valuable in obtaining tighter constraints (Bahcall *et al* 1992).

Lower mass objects can be constrained by high resolution observations. Using a sample of VLBI observations of compact radio sources, Kassiola, Kovner & Blandford (1991) have excluded a mass fraction $\Omega \gtrsim 0.4$ of compact objects in the mass range $10^7M_\odot \lesssim M \lesssim 10^9M_\odot$. In principle, using a homogeneous sample of compact radio sources, the mass range can be lowered to about $10^5M_\odot$, and a sample of about 1000 objects can limit Ω in that mass range to better than 0.01.

If the dark matter in galaxies is made of high mass black holes with $M \sim 10^6M_\odot$, their presence should show up in high-resolution VLBI observations of multiply imaged QSOs (Wambsganss & Paczyński 1992), as they would leave an imprint on the VLBI maps which can be detected by comparing the milliarcsecond structure of the images. Compact objects of about a solar mass can in principle be detected by their microlensing power, leading to lens-induced variability. But, as discussed in Sect. 1.4, it is extremely difficult to distinguish this effect from intrinsic variability. If gamma-ray bursts originate from sources at cosmological distances, for which the evidence is now accumulating (e.g., Mao & Paczyński 1992), lensing of a burst source by a compact object will lead to two images, which cannot be spatially resolved by gamma-ray telescopes, but they can be resolved in time: the time delay is about $50(M/M_\odot)$ seconds. Hence, a cosmologically significant density of compact lenses in the appropriate mass range can be detected from recurrent bursts (see Mao 1992, Narayan & Wellington 1992 for details).

4.6. Dark matter on large scales

The universe is inhomogeneous on scales larger than galaxy clusters; however, the mass distribution on such large scales is no longer sufficiently compact to yield strong lensing events. Still, it may be possible to detect the impact of such large scale inhomogeneities on the propagation of light rays. At least two such possibilities have been discussed recently in the literature.

A light bundle propagating through the universe is affected by the shear (Weyl focusing) produced by the inhomogeneities. Thus, an intrinsically round source will attain a slight ellipticity. So far, the situation is similar to the formation of arclets in clusters, except that here no 'center of gravity' can be identified in general. But, as demonstrated in Blandford *et al* (1991, see also Miralda-Escudé 1991b, Kaiser 1992), the shear of large-scale inhomogeneities will lead to a nonzero two-point correlation function of the ellipticities of images from high-redshift sources. The sky is fairly densely covered with faint galaxies, which are supposed to have redshifts $\gtrsim 1$ (Tyson 1988); this source population is thus the natural candidate for such an investigation, which, due to the faintness of the galaxies and their intrinsic ellipticities will be difficult to carry out. The shape of the two-point correlation function reflects the spectrum of the inhomogeneities of large-scale matter in the universe.

Another method for detecting large-scale matter inhomogeneities has been recently pointed out by Bartelmann & Schneider (1992). Motivated by the claim of Fugmann (1990) that there is a large-scale density excess of galaxies from the Lick catalogue around high-redshift flat-spectrum radio sources, we studied the lensing effect of the large-scale matter distribution in the universe on high-redshift objects. Although the corresponding magnifications are very small, they can be detected in a statistically significant way if the source population has a steep intrinsic luminosity function (or if multiple waveband amplification bias is taken into account, see Borgeest, von Linde & Refsdal 1991). In this case, the sources will be preferentially observed behind overdense structures. If one now assumes (as is generally done) that galaxies find themselves in overdense regions, they trace the overdensities and a large-scale correlation of high-redshift sources and galaxies is expected. These effects are, however, tedious and require robust statistical methods to extract them from observations.

4.7. The size of Lyα clouds

Each QSO at sufficiently high redshift, such that the Lyα emission line can be observed from Earth, shows a large number of narrow absorption lines shortward of the Lyα emission line. This so-called 'forest' is interpreted as being due to intervening material in the line-of-sight to the QSO, and the absorption lines being due to the Lyα transition. It is less clear what the nature of the absorbers is; one can measure the redshift, equivalent width (yielding the column density of neutral hydrogen) and line width. Gravitational lens systems provide us with an invaluable tool to determine the size of this absorbing material.

Consider a lens system in which a high-redshift QSO has two observable images. The transverse separation between the corresponding light bundles varies as a function of redshift: it is zero at the source, and largest at the redshift of the lens. Suppose an absorption line is seen in the spectra of both images, at the same redshift; then the size of the absorbing material must be at least as large as the separation between the two light bundles at the respective redshift. Hence, redshift coincidences of absorption

lines leads to a lower bound on the size of the absorbing material. If, in addition, the equivalent widths of the corresponding lines in both spectra are strongly correlated, it could be concluded that the two light bundles actually have crossed the same cloud (as opposed to crossing two different clouds at the same redshift).

Two lens systems have turned out to be useful for such studies. As mentioned above, the lensing nature of one of them, 2345+007, has not yet been totally clarified, but it is an excellent candidate system. The large angular separation of 7.3 arcseconds makes this a very useful target for these spectroscopic investigations (Foltz *et al* 1984), although the faintness of the QSO images renders such an investigation difficult. If this is indeed a lens system, and if the lens redshift is 1.49 as suggested by the strong iron absorption at this redshift, the size of Lyα clouds can be estimated to be $10\,\mathrm{kpc} \lesssim R \lesssim 20\,\mathrm{kpc}$ (Bajtlik, personal communication). A second system, UM673 with an image separation of 2.2 arcseconds, is brighter and thus higher-quality spectroscopy can be obtained. Results of such a study are reported in Smette *et al* (1992); due to the smaller image separation, only sharp lower limits can be obtained, which are completely compatible with the value quoted above.

One can turn this argument around: suppose the size of the Lyα clouds were known; then, a correlation analysis of the absorption line spectra of multiple QSOs could be used to decide whether the multiple system is due to lensing. Note that for this kind of argument, the size of the clouds need to be known only approximately, since the transverse separation of light rays corresponding to multiple QSO images differs greatly for physical pairs of QSOs and for lensed sources. Thus, this Lyα diagnostics may turn out to be the most powerful tool to decide about the lensing nature of multiple QSO systems.

5. Concluding remarks

The investigation of gravitational lensing has provided us with a powerful tool in extragalactic astronomy. Currently, the interplay of observations and theory is most fruitful for both: lensing has triggered renewed interest in old topics like simple geometrical optics or light propagation in curved spacetime, whereas on the other hand, theoretical predictions can be tested observationally only if highest quality data are obtained. It is possible that gravitational lensing effects (microlensing) will shed light on the structure of QSOs and can yield interesting cosmological information, most noticibly about the Hubble constant. The history of gravitational lensing has provided us with quite a few surprises – arcs were not predicted, for example – and some visionary ideas have come true finally, such as the detection of microlensing, first predicted by Chang and Refsdal in 1979. On the other hand, we see a great potential of applying statistical lensing to well-defined samples of sources once these become available. Whatever the main direction of future research in lensing, exciting results can be anticipated.

References

Bahcall, J.N. *et al* : 1992, ApJ 387, 56.
Bartelmann, M. & Schneider, P.: 1992, AA submitted.
Bergmann, A.: 1992, PhD Thesis, Stanford University.
Blandford, R.D. & Narayan, R.: 1986, ApJ 310, 568.

Blandford, R.D. & Narayan, R.: 1992, Ann. Rev. Astr. Ap. (in press)(BN).
Blandford, R.D., Saust, A.B., Brainerd, T.G. & Villumsen, J.V.: 1991, MNRAS 251, 600.
Borgeest, U.: 1986, ApJ 309, 467.
Borgeest, U., von Linde, J. & Refsdal, S.: 1991, AA 251, L35.
Burke, W.L.: 1981, ApJ 244, L1.
Chang, K. & Refsdal, S.: 1979, Nature 282, 561.
Corrigan, R.T. *et al* : 1991, Astron. J. 102, 34.
De Rujula, A., Jetzer, Ph. & Masso, E.: 1992, AA 254, 99.
Dyer, C.C. & Roeder, R.C.: 1973, ApJ 180, L31.
Ehlers, J. & Schneider, P.: 1986, AA 168, 57.
Falco, E.E., Gorenstein, M.V. & Shapiro, I.I.: 1991, ApJ 372, 364.
Filippenko, A.B.: 1989, ApJ 338, L49.
Foltz, C.B., Weymann, R.J., Röser, H.-J. & Chaffee, F.H.: 1984, ApJ 281, L1
Foltz, C.B., Hewett, P.C., Webster, R.L. & Lewis, G.F.: 1992, ApJ 386, L43.
Fort, B.: 1990, in: *General Relativity and Gravitation*, Ashby, N., Bartlett, D.F. & Wyss, W. (eds.), Cambridge University Press.
Fugmann, W.: 1990, AA 240, 11.
Fukugita, M., Futamase, T., Kasai, M. & Turner, E.L.: 1992, ApJ 393, 3.
Fukugita, M. & Turner, E.L.: 1991, MNRAS 253, 99.
Futamase, T. & Sasaki, M: 1989, Phys. Rev. D 40, 2502.
Futamase, T.: 1989, MNRAS 237, 187
Gorenstein, M.V. *et al* : 1988, ApJ 334, 42.
Gorenstein, M.V., Falco, E.E. & Shapiro, I.I.: 1988, ApJ 327, 693.
Gott, J.R., Park, M.-G. & Lee, H.M.: 1989, ApJ 338, 1.
Grieger, B.: 1990, in: Mellier *et al* 1990, p.198.
Hammer, F. & Le Fevre, O.: 1990, ApJ 357, 38.
Hammer, F. & Le Fevre, O.: 1991, ESO Messenger 63, 59.
Hewitt, J.N. *et al* : 1988, Nature 333, 537.
Huchra, J. *et al* : 1985, Astron. J. 90, 691.
Jacobs, M.W., Linder, E.V. & Wagoner, R.V.: preprint Stanford, ITP–905
Jaroszyński, M., Wambsganss, J. & Paczyński, B.: 1992, preprint.
Kaiser, N.: 1992, ApJ 388, 272.
Kassiola, A., Kovner, I. & Blandford, R.D.: 1991, ApJ 381, 6.
Kayser, R. & Schramm, T.(ed.): 1992, *Proceeding of the Hamburg conference on gravitational lensing*, Springer-Verlag (in press).
Kent, S.M. & Falco, E.E.: 1988, Astron. J. 96, 1570.
Kochanek, C.S.: 1990, MNRAS 247, 135.
Kochanek, C.S.: 1991a, ApJ 382, 58.
Kochanek, C.S.: 1991b, ApJ 379, 517.
Kochanek, C.S.: 1992, ApJ 384, 1.
Kochanek, C.S., Blandford, R.D., Lawrence, C.R. & Narayan, R.: 1988, MNRAS 238, 43.
Kochanek, C.S. & Narayan, R.: 1992, preprint.
Langston, G.I. *et al* : 1990, Nature 344, 43.
Magain, P., Surdej, J., Vanderriest, C., Pirenne, B. & Hutsemekers, D.: 1992, AA 253, L13.
Mao, S.: 1991, ApJ 380, 9.
Mao, S.: 1992, ApJ 389, L41.
Mao, S. & Paczyński, B.: 1992, ApJ, submitted.
Maoz, D. *et al* : 1992, ApJ 386, L1.
McKenzie, R.H.: 1985, J. Math. Phys. 4, 1194.
Mellier, Y., Fort, B. & Soucail, G.(ed.): 1990, *Gravitational Lensing*, Lecture Notes in Physics 360, Springer-Verlag (Berlin).
Miralda-Escudé, J.: 1991a, ApJ 370, 1.
Miralda-Escudé, J.: 1991b, ApJ 380, 1.
Moran, J.M., Hewitt, J.N. & Lo, K.Y.(ed.): 1989, *Gravitational Lenses*, Lecture Notes in Physics 330, Springer-Verlag (Berlin).
Narayan, R.: 1992, in: Kayser & Schramm 1992.
Narayan, R. & Schneider, P.: 1990, MNRAS 243, 192.

Narayan, R. & Wellington, S¿: 1992, ApJ, in press.
Nieto, J.-L. *et al* : 1988, ApJ 325, 644.
Ostriker, J.P. & Vietri, M.: 1985, Nature 318, 446.
Paczyński, B.: 1986, ApJ 304, 1.
Paczyński, B.: 1991, ApJ 371, L63.
Perlick, V.: 1990, Class. Quantum Grav. 7, 1319.
Press, W.H. & Gunn, J.E.: 1973, ApJ 185, 397.
Press, W.H., Rybicki, G.B. & Hewitt, J.N.: 1992a, ApJ 385, 404.
Press, W.H., Rybicki, G.B. & Hewitt, J.N.: 1992b, ApJ 385, 416.
Rauch, K. & Blandford, R.D.: 1991, ApJ 381, L39.
Refsdal, S.: 1964, MNRAS 128, 307.
Rix, H.-W., Schneider, D.P. & Bahcall, J.N.: 1992, ApJ, in press.
Roberts, D.H. *et al* : 1985, ApJ 293, 356.
Schild, R. & Smith, R.C.: 1991, Astron. J. 101, 813.
Schneider, P.: 1984, AA 140, 119.
Schneider, P., Ehlers, J. & Falco, E.E.: 1992, *Gravitational Lenses*, Springer-Verlag (New York)(SEF).
Schneider, P. & Wambsganss, J.: 1990, AA 237, 42.
Seitz, S. & Schneider, P.: 1992, AA (submitted).
Sommerfeld, A.: 1959, *Vorlesungen über Theoretische Physik, Bd.IV. Optik*, Geest & Portig (Leipzig.
Smette, A. *et al* : 1992, ApJ 389, 39.
Stickel, M., Fried, J. & Kühr, H.: 1988a, AA 198, L13.
Stickel, M., Fried, J. & Kühr, H.: 1988b, AA 206, L30.
Stickel, M., Fried, J. & Kühr, H.: 1989, AA 224, L27.
Stockton, A.: 1980, ApJ 242, L141.
Turner, E.L., Cen, R. & Ostriker, J.P.: 1992, AJ 103, 1427.
Tyson, J.A.: 1988, Astron. J. 96, 1.
Tyson, J.A., Valdes, F. & Wenk, R.A.: 1990, ApJ 349, L1.
Walsh, D.: 1989, in: Moran *et al* 1989, p.11.
Wambsganss, J.: 1990, *Gravitational Microlensing*, Ph.D. Thesis, University of Munich, available as MPA report 550.
Wambsganss, J. & Paczyński, B.: 1992, preprint.
Wambsganss, J., Paczyński, B. & Schneider, P.: 1991, ApJ 358, L33.
Whitney, H.: 1955, Ann. Math. 62, 374.
Witt, H.J., Kayser, R. & Refsdal, S.: 1992, AA, submitted.
Wu, X.P. & Hammer, F.: 1992, preprint.
Yee, H.K.C.: 1988, Astron. J. 95, 1331.
Young, P. *et al* : 1980, ApJ 241, 507.